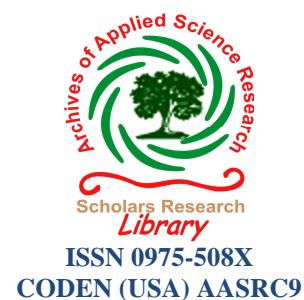




Scholars research library

Archives of Applied Science Research, 2011, 3 (5):144-154
(<http://scholarsresearchlibrary.com/archive.html>)



Influence of rare earth metal dopant (Nd^{3+}) on the thermal, mechanical and optical properties of L-Arginine Acetate Single Crystals

M. Arul Thalpathi¹, P. Gnanasekaran², V. Santhanam³ and K. Thamizharasan^{4*}

¹Department of Physics, Government Arts College, Nandanam, Chennai

²Department of Physics, C. Kandaswami Naidu College, Chennai

³Department of Physics, Presidency College, Chennai

⁴Department of Physics, Sir Theagaraya College, Chennai

ABSTRACT

Single crystals of pure and Neodymium (Nd^{3+}) doped L-Arginine Acetate (LAA) were grown successfully by slow evaporation technique. In the present study, to improve the device characteristics of LAA crystals, metal dopant was incorporated into the pure crystals. The grown pure and doped LAA crystals were confirmed by X-ray powder diffraction studies. The pure and doped crystals were characterized by Fourier Transform Infrared (FT-IR), Fourier Transform Raman (FT-Raman) and Thermal studies. Absorptions of the grown crystals were analyzed using UV-Vis-NIR studies which revealed that these crystals possess minimum absorption from 250 nm to 1650 nm. Further, it was found that the optical properties were enhanced by the incorporation of the dopant. Hardness, dielectric and photoconductivity studies were also carried out for the pure and doped LAA crystals. Nonlinear optical studies of pure and doped crystals were carried out and it revealed that the dopant has increased the efficiency of the pure LAA crystal.

INTRODUCTION

Nonlinear optical (NLO) organic materials play an important role for optical second harmonic generation (SHG) due to their applications in the domain of optoelectronics and photonics [1, 2]. Amino acids are strong candidates for optical SHG because they contain chiral carbon atom and crystallize in non-centrosymmetric space groups. Recent studies reveal that L-arginine acetate (LAA) possesses excellent optical, thermal and mechanical properties, which make it a strong candidate for photonic device fabrications [3]. Morphological analysis of LAA crystal indicates its growth as a polyhedron with 16 developed faces, among which the (100) face is the most prominent one [4]. The powder SHG efficiency of LAA was found to be three times that of KDP [5]. The present investigation deals with the growth of pure LAA and metal doped LAA crystals by slow solvent evaporation technique. The grown crystals are subjected to powder XRD to estimate the crystal structure and space group. The content of the dopant was determined by ICP analysis. FT-IR, FT-Raman, UV-Vis-NIR, thermal and microhardness studies were carried out for the grown pure and doped crystals. The SHG efficiency of the pure and doped LAA crystals

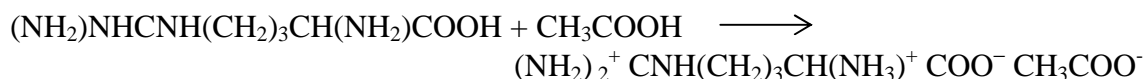
were also studied using Nd:YAG Q-switched laser.

MATERIALS AND METHODS

Experimental Procedures

2. 1 Synthesis and solubility

Equimolar quantity of AR grade L-arginine and acetic acid were taken and dissolved in double distilled water to prepare the aqueous solution of LAA. The reaction that takes place between L-arginine and acetic acid in water medium is as follows:



The synthesized product was allowed to evaporate in a petri dish and it was later collected in the form of salt. The growth of metal substituted crystal is achieved by using the same procedure by adding dopant of 2 mol % concentration of Nd^{3+} to the LAA solution. The synthesized salt of pure and doped LAA was utilized for the measurement of its solubility in water. The solubility of pure and doped LAA in double distilled water was measured at six different temperatures (30, 35, 40, 45 50 and 55°C) using a constant temperature bath of accuracy ± 0.01 °C [6]. The amount of LAA salt dissolved in 100 ml of water at the above mentioned temperatures has been plotted as a function of temperature (Figure 1). From the solubility curve, it is observed that the solubility of both pure and doped samples of LAA increases with increase in temperature. The incorporation of dopant into the parent solution has promoted the growth rate of the crystals. Bulk crystals were grown by successive recrystallisation and the crystals are found to be transparent and free from defects. Figure 2 shows the photograph of as grown pure and doped crystals in a period of 50 days.

RESULTS AND DISCUSSION

3.1 Powder XRD studies

Powder X-ray diffraction studies of pure and doped LAA crystals were carried out using Rich Seifert, XRD 3000P, X-ray diffractometer with $\text{Cu K}\alpha$ ($\lambda = 1.54056$ Å) radiation. The samples were scanned for 2θ values from 10° to 50° at a rate of $2^\circ/\text{min}$. Figure 3.3 shows the Powder XRD pattern of the pure and doped LAA crystals.

The powder patterns were indexed and the lattice parameter values for the pure and doped LAA crystals were calculated by fitting the XRD data with “least square method” using “XRDA” program. It is observed that both the pure and doped crystals crystallize in Monoclinic P2_1 space group. The lattice parameters of the samples are presented in Table 1 and agree well with the reported values [5]. There are slight variations in the lattice parameters and cell volume of the pure and doped crystals. These variations are due to the incorporation of the dopant in the LAA crystal lattice.

3.2 Inductively coupled plasma analysis

In order to determine the weight percentage of doped LAA crystal, 10 mg of fine powder of the crystal was dissolved in 100 ml of triple distilled water. This prepared solution was taken for the ICP analysis. The results obtained from ICP show that 1.03% of Nd^{3+} ($103 \mu\text{g}/100\text{ml}$) was present in the solution. It is observed that the amount of dopant incorporated into the crystal lattice is below its original concentration (2%) in the solution.

3.3 FT-IR analysis

The middle infrared spectra of pure and doped L-arginine acetate are shown in Figure 4. Both the pure and doped compounds show absorption at 1620 cm^{-1} indicating the presence of primary amino group. The spectrum of LAA shows a stretching strong absorption at 1550 cm^{-1} which is characteristic of acyclic -NH stretching and O-H stretching. The FT-IR spectra of both the pure and doped LAA confirm the structural aspects of pure compounds. The spectral assignments of both the crystals are given in Table 2.

Doping of metal ion into the crystal lattices does not show any significant change in absorption pattern. Some of the absorptions show a marked difference in percentage transmittance. The percentage changes of transmittance are worth noting. It is inferred that the metal ion form weak linkages in the interstices of the corresponding crystals. The broad absorption around 3000 cm^{-1} indicates the presence of both C=O stretching and O-H stretching.

3.4 FT- Raman Spectra

The FT-Raman spectra of pure and doped LAA are shown in Figure 5. It is a confirmatory evidence for the presence of the metal dopant in the lattice of L-arginine acetate crystal. The N-H stretching frequencies are found between 3100 cm^{-1} and 2600 cm^{-1} in the form of a broad strong band with multiple peaks. The characteristic band at 1579 cm^{-1} is due to the asymmetric N-H deformation. The weak absorption band observed at 3065 cm^{-1} shows the N-H stretching of amino group. It is inferred from the spectra that the peaks at 1415 cm^{-1} and 1626 cm^{-1} are due to the C=O stretching of carboxylic group. The Nd^{3+} -LAA spectra shows that absence of peak at 2125 cm^{-1} which may be responsible for metal linkage with N of amino group. The FT-Raman spectral assignments are shown in Table 3.

3.5 UV-Vis-NIR spectrum

Optical absorption data were taken on these polished crystal samples of about 4mm to 6mm thickness using a Varian carry 5E model dual beam spectrophotometer between 200nm – 2500nm. The spectra (Figure 6) indicate that the pure and doped LAA crystals have minimum absorption in the entire visible region. The cut-off wavelengths for pure and doped crystals are 265nm and 249nm respectively. Interestingly the doped crystal has reduced absorption and reduced cut-off wavelength. Moreover the Nd^{3+} doped crystal shows an improved transparency window. The required properties for NLO activity are minimum absorption and low cut-off wavelength. These properties are improved in the doped crystal. Both the pure and doped crystals possess good transparency for the wavelengths of sources which are used for photonic devices. It is found that these crystals possess a good transparency for the wavelengths of sources that are commonly employed for SHG, such as Nd:YAG (1064 nm), InGaAsP (1200–1550 nm), GaAs (820–850 nm) [7].

3.6 Microhardness studies

Hardness of the material is a measure of resistance, it offers to deformation [8]. Microhardness behaviour of pure and doped LAA single crystal was tested by employing Vickers microhardness tester. Measurements were taken by varying the applied load from 10g to 50g. As micro cracks were developed at higher loads, the maximum applied load was restricted to 50g only. The plot of variations of Vickers hardness number with applied load for (100) plane of pure and doped LAA are shown in Figure 7. From the plot, it can be noted that the hardness of the crystal decreases with increasing load both for pure and doped samples. The decrease of the microhardness with the increasing load is in agreement with the normal indentation size effect (ISE). The hardness number Hv has improved in the case of doped crystal.

3.7 Thermal studies

The thermo gravimetric analysis of LAA was carried out between 23°C and 1200°C in nitrogen atmosphere at a heating rate of 10K/min. The resulting TGA and DTG traces are shown in Figure 8. Both the pure and doped crystals show two stages of weight loss, 76.42% and 77.92% in the first stage and 23.72% and 19.21% in the second stage for pure and doped crystal respectively. The decomposition starts at 232.9°C and 228.1°C respectively for pure and doped samples. Both the thermogram show negligible residue. The decrease in decomposition temperature of the doped crystal is due to the decrease in bond energy by the addition of Nd^{3+} .

3.6 NLO studies

Kurtz and Perry powder SHG test was carried out on pure and doped LAA single crystals to study its NLO properties [9]. The sample was illuminated using Q-switched, mode locked Nd:YAG laser with input pulse of 6.2 mJ. The emission of green radiation from the crystal confirmed the second harmonic signal generation in the crystal. The second harmonic signal of 830 mW and 1320 mW respectively were obtained for pure and doped LAA with reference to KDP (275 mW). Thus, the SHG efficiency of pure and doped LAA crystals is 3.0 and 4.8 times more than that of KDP. Thus, the Nd^{3+} has increased the efficiency of pure LAA.

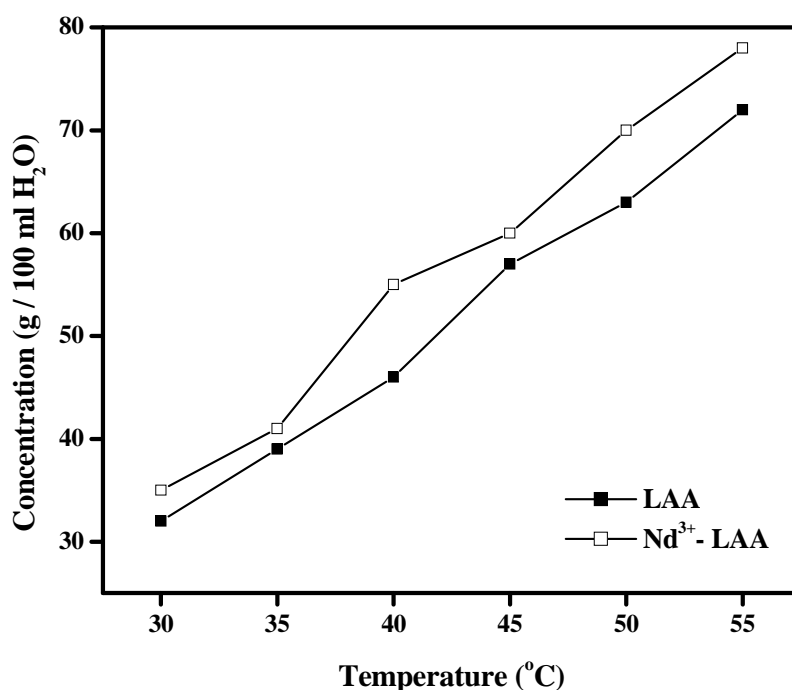


Figure 1 Solubility curves of pure and Nd^{3+} doped LAA crystal

3.9 Dielectric studies

The capacitance of the sample was noted for the applied frequency that varies from 100 Hz to 5 MHz at room temperature. Figure 9 shows the plot of dielectric constant versus applied frequency of pure and doped LAA. The applied frequency has been represented by logarithmic values in the plot. The dielectric constant has high values in the lower frequency region and then it decreases with the applied frequency and increases with different temperatures. This is due to the presence of space charge polarization which depends on purity and perfection of the sample. Displacement of an ion from an equilibrium position is equivalent to the placing of the fictitious dipole at the state with the ion in equilibrium. Although positive and negative ions displace in

opposite directions in an electric field, the induced moments all have the same sign. Since ionic polarization is related to the oscillation of ions, the proper frequencies are much lower than those of electrons due to large differences between masses [10]. The dielectric loss is also studied as a function of frequency. The curves are shown in Figure 10, suggesting that the dielectric loss is strongly dependent on the frequency of the applied field, similar to that of the dielectric constant. This behaviour is common in the case of ionic systems. The low value of dielectric loss indicates that the grown pure and doped LAA crystals have lesser defects.

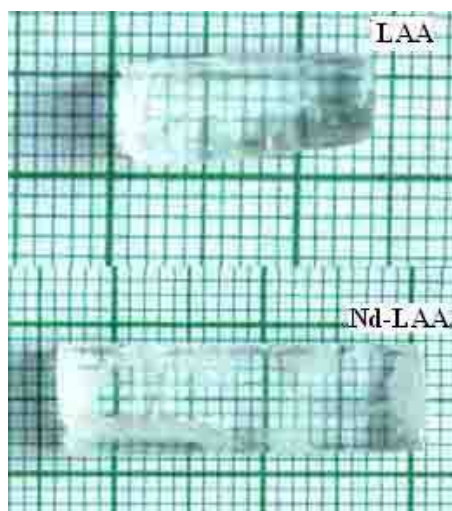


Figure 2 Photograph of as grown pure and Nd^{3+} doped LAA crystal

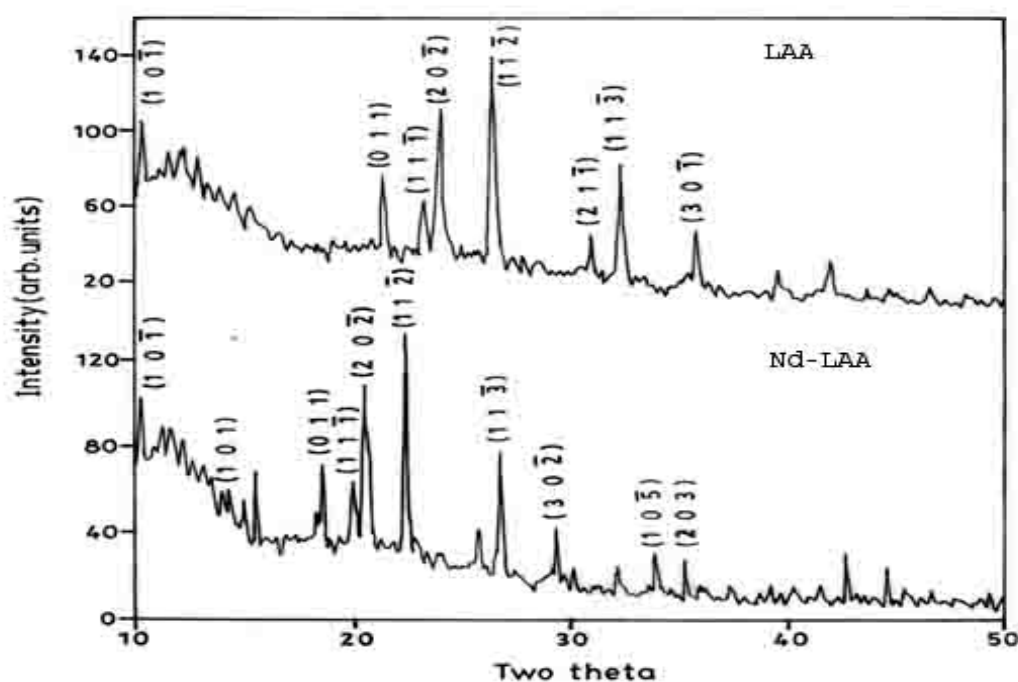


Figure 3 Powder XRD pattern of pure and Nd^{3+} doped LAA crystal

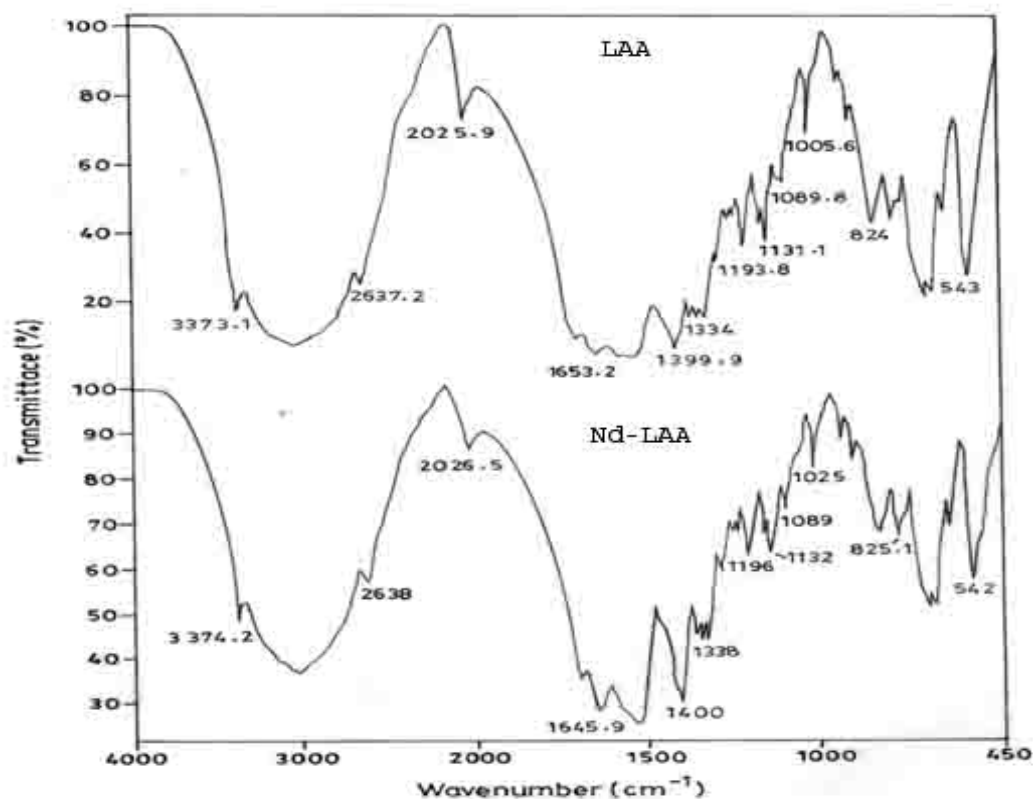


Figure 4 FT-IR spectrum of pure and Nd³⁺ doped LAA crystal

3.10 Photoconductivity studies

Photoconductivity studies were carried out at room temperature for the pure and doped LAA crystals, using Keithley 485 picoammeter. Dark current and photocurrent are measured for various values of applied electric field. The plots of photocurrent and dark current as a function of the applied field for pure and Nd³⁺ doped LAA crystals are as shown in Figure 11. It is observed from the plots that the photocurrent is always higher than the dark current, hence it is concluded that both pure and doped LAA exhibit positive photoconductivity [11].

Table 1 Lattice parameters for pure and Nd³⁺ doped LAA crystal

Lattice parameters	Pure LAA	La ³⁺ -LAA
a (Å)	9.209	9.122
b (Å)	5.201	5.252
c (Å)	13.101	12.801
α(°)	90	90
β(°)	108.91	107.54
γ(°)	90	90
Crystal System	Monoclinic	Monoclinic
Space group	P2 ₁	P2 ₁
Volume (Å ³)	586.20	581.38

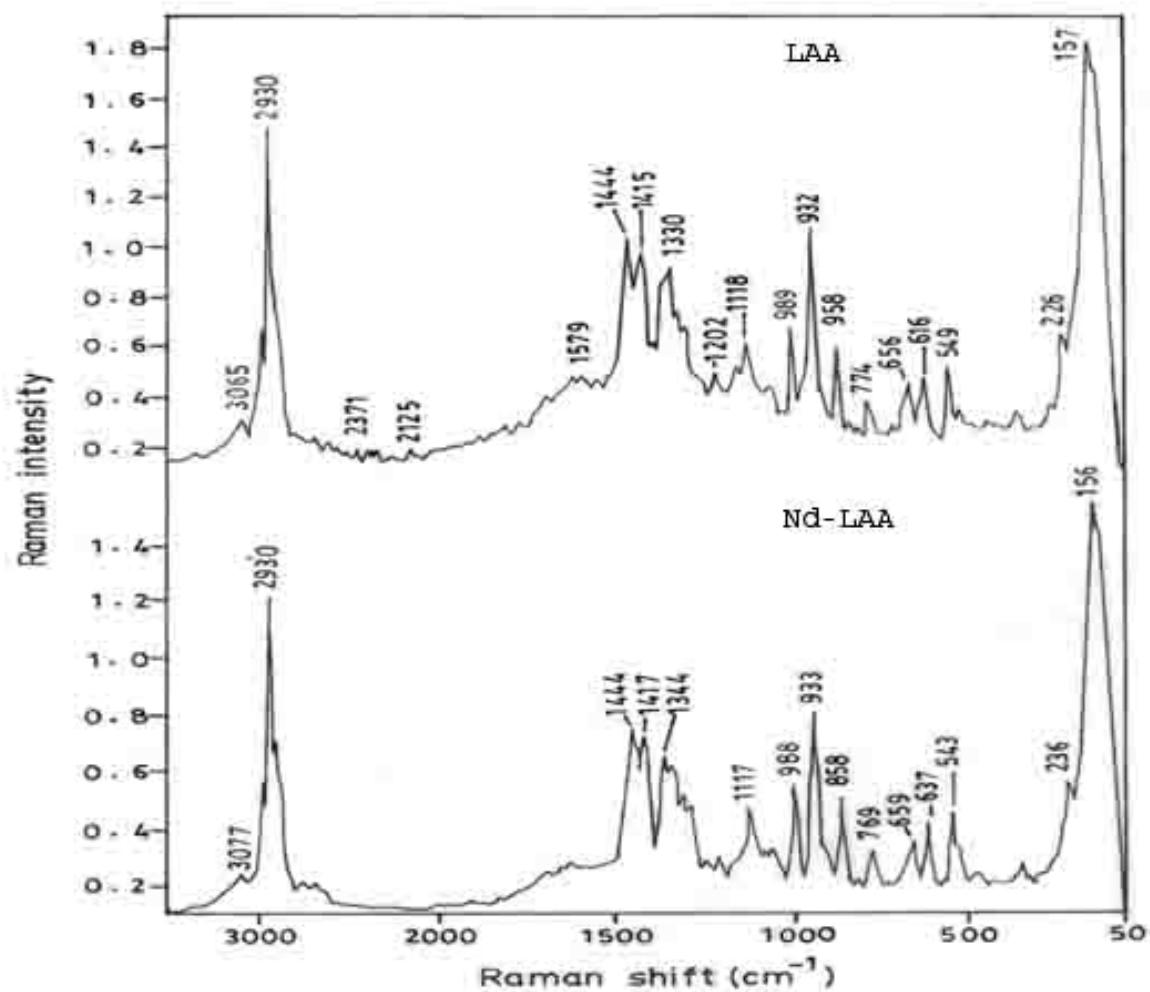


Figure 5 FT-Raman spectrum of pure and Nd³⁺ doped LAA crystal

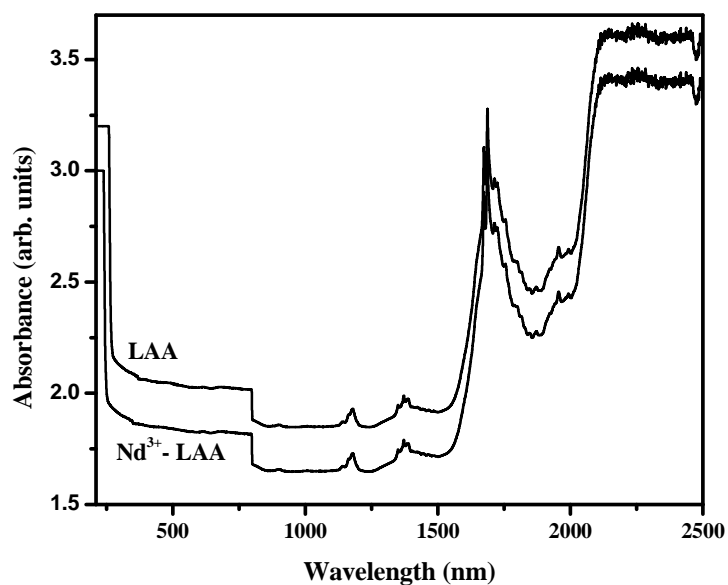


Figure 6 Absorption spectrum of pure and Nd³⁺ doped LAA crystal

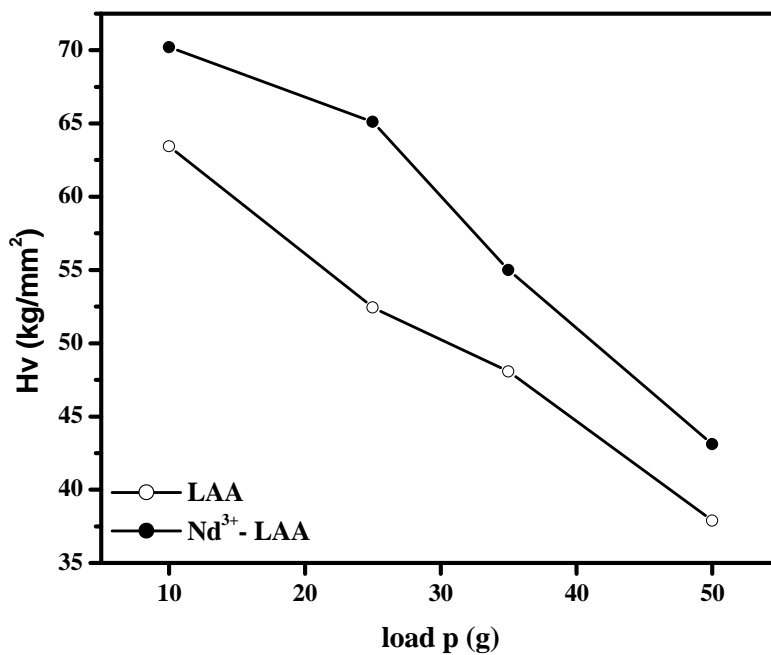


Figure 7 Variation of Hv with load for pure and Nd³⁺ doped LAA crystal

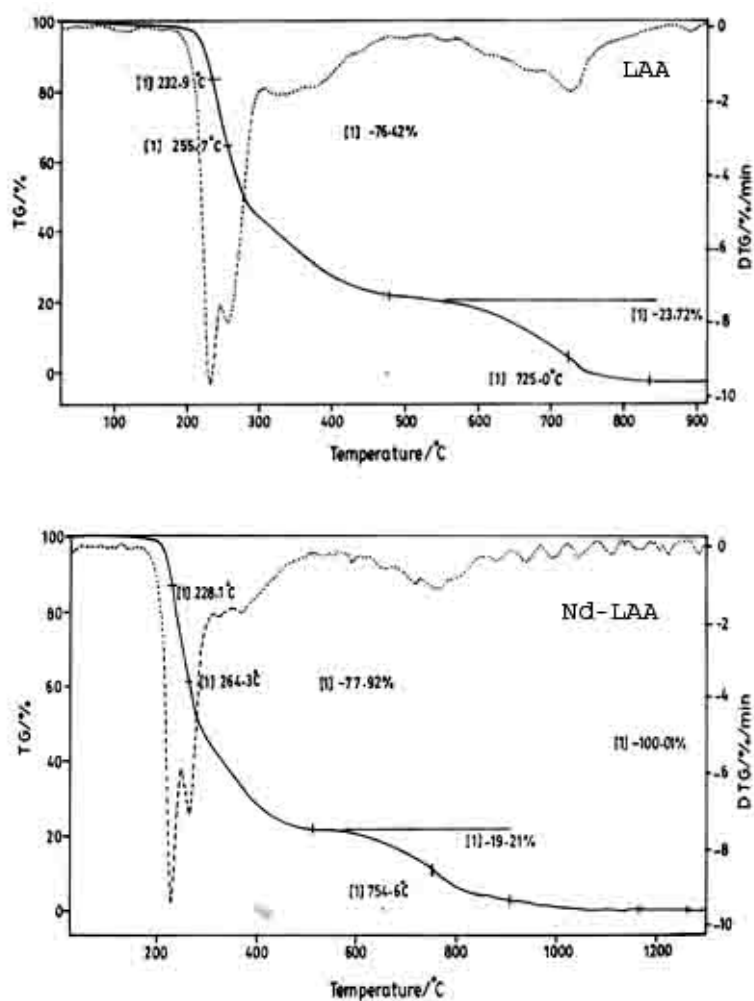


Figure 8 TGA and DTG curves of pure and Nd³⁺ doped LAA crystal

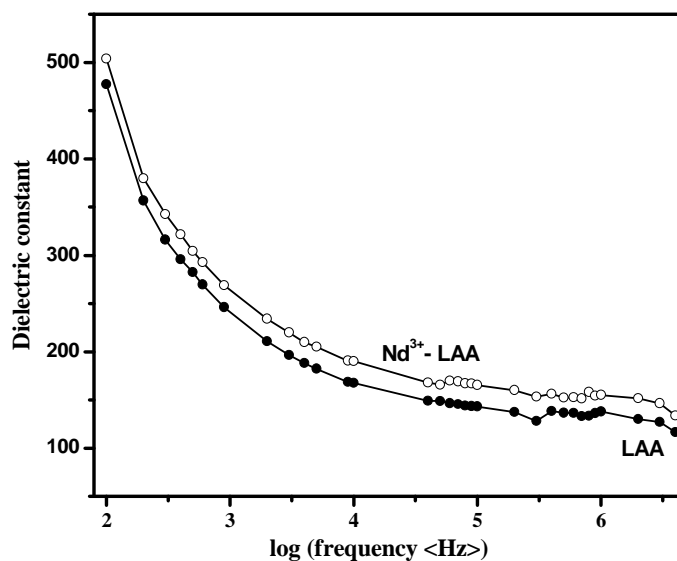


Figure 9 Variation of Dielectric constant for pure and Nd^{3+} doped LAA crystal

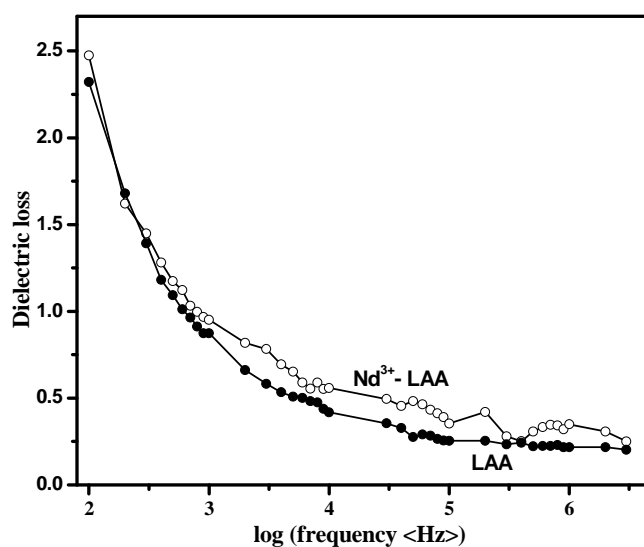


Figure 10 Variation of Dielectric loss for pure and Nd^{3+} doped LAA crystal

Table 2 FT-IR spectral assignments of pure and Nd^{3+} doped LAA crystal

Wave number (cm^{-1})		Assignments
Pure LAA	Nd^{3+} -LAA	
3750 - 2300	3750 - 2300	NH and CH stretching vibration
1532	1531	COO^- asymmetric stretching
1400	1400	COO^- symmetric stretching
1228, 1197	1229, 1196	COO^- vibration
1093	1089	C-N stretching
928	929	CH_2 rocking
890	891	C-C stretching
670	669	NH_2 out of plane

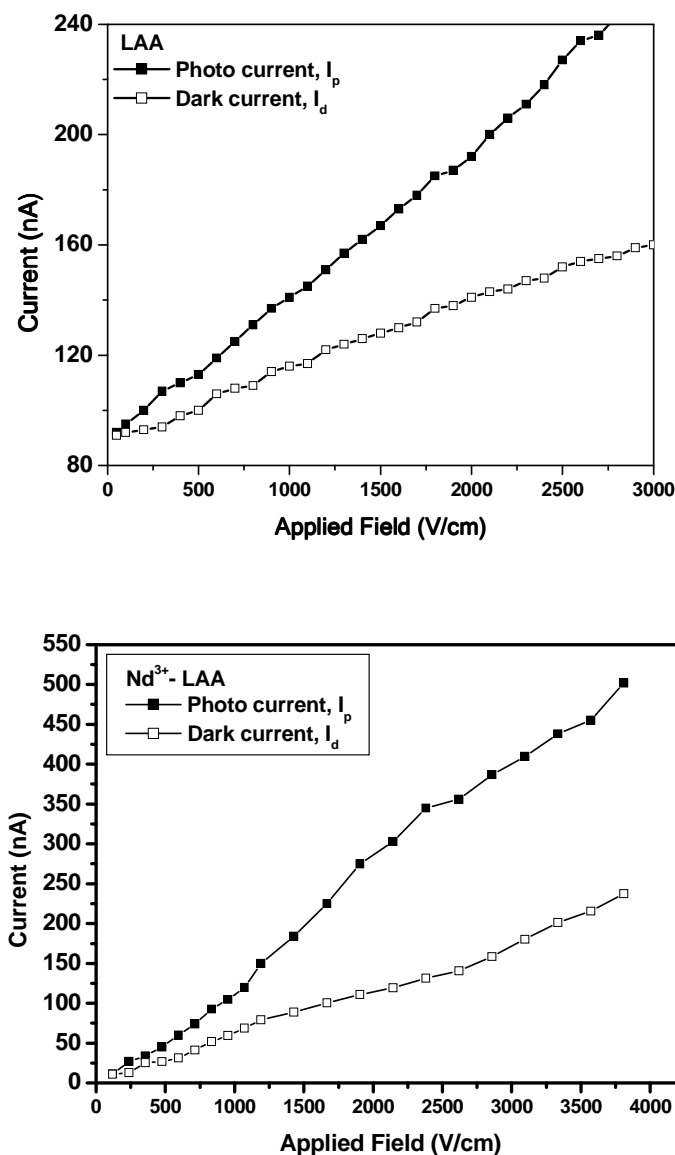


Figure 11 Field dependant conductivity of pure and Nd^{3+} doped LAA crystal

Table 3 FT-Raman spectral assignments of pure and Nd^{3+} doped LAA crystal

Wave number (cm^{-1})		Assignments
Pure LAA	Nd^{3+} -LAA	
2965	2964	Aliphatic CH_3
2930	2930	Aliphatic CH_2
2125	-	C=C stretching vibration
1626	1626	Asymmetric C=O stretching
1579	1578	N-H asymmetric deformation
1415	1417	Symmetric C=O stretching
1330	1344	CH_3 symmetric deformation

CONCLUSION

In the present work, the growth of promising NLO crystal of both pure and Nd^{3+} doped LAA single crystals were achieved by slow evaporation technique. Powder X-ray diffraction studies

were carried out, and the lattice parameters were determined. The presence of functional groups in pure and Nd³⁺ doped LAA were analyzed by FT-Infrared and FT-Raman studies. The UV-Vis-NIR spectra of the pure and doped LAA shows good optical transmittance in the entire visible region and the dopants have increased the percentage of transmission in LAA. The SHG efficiency of both pure and doped LAA was found to be higher than that of KDP. The thermal studies of pure LAA reveal that the decomposition of pure LAA starts at 232.9°C. The role of dopant in the pure LAA has marginal influence on the thermal properties of LAA. It can be noted that the hardness of the crystal decreases with increasing load for both pure and doped samples. The dielectric studies reveal the low value of dielectric constant / dielectric loss of the crystal at high frequency region. The photoconductivity studies of both pure and doped LAA confirm the positive photoconducting nature of the sample.

REFERENCES

- [1] Madhavan J., Aruna S., Ambujam K., Joseph Arul Prakasam A., Ravikumar S.M., Gulam Mohamed M. and Sagayaraj P., *Cryst. Res. Technology*, 41, 1211-1216 (2006).
- [2] Madhavan J., Aruna S., Anuradha A., Prem Anand D., Vetha Potheher I., Thamizharasan K. and Sagayaraj P., *Optical Materials*, 29, 1211-1216 (2007).
- [3] Tanusri Pal, Tanusree Kar, *Materials Chemistry and Physics*, 91, 343-347 (2005).
- [4] Tanusri Pal, Tanusree Kar, Gabriele Bocelli and Lara Rigi. (2003), *Crystal Growth and Design*, 3, 13 -16 (2003).
- [5] Muralidharan R., Mohankumar R., Jayavel R. and Ramasamy P. (2003), *J. Crystal Growth*, 259, 321–325 (2003).
- [6] Praveen Kumar P., Manivannan V., Tamilselvan S., Senthil S., Victor Antony Raj., Sagayaraj P. and Madhavan J. (2008), *Optics Communications*, 281, 2989-2995 (2008).
- [7] J.J. Rodrigues Jr., L. Misoguti, F.D. Nunes, C.R. Mendonc_a, S.C. Zilio, *Optical Materials* 22, 235–240 (2003).
- [8] Sankar D., Praveen Kumar P and Madhavan J (2010) *Physica B*, 405, 1233-1238 (2010)
- [9] S.K. Kurtz, T.T. Perry, *J. Appl. Phys.* 39, 3798 (1968).
- [10] Bunget and Popescu M. (1984), 'Physics of Solid Dielectrics', Elsevier, New York.
- [11] Joseph Arul Pragasam A., Madhavan J., Gulam Mohamed M., Selvakumar S., Ambujam K., and Sagayaraj P., *Optical Materials*, 29, 173-179 (2006).